Optimization of attenuation and scatter corrections in sentinel lymph node scintigraphy using SPECT/CT systems

doi: 10.1007/s12149-014-0939-1

Original Article

Optimization of attenuation and scatter corrections in sentinel lymph node scintigraphy using SPECT/CT systems

Hiroto Yoneyama[1], Hiroyuki Tsushima[2], Masahisa Onoguchi[3],Takahiro Konishi[1], Kenichi Nakajima[4], Shinro Matsuo[4], Daiki Kayano[4], Hiroshi Wakabayashi[4], Anri Inaki[4], Seigo Kinuya[4]

1 Department of Radiological Technology, Kanazawa University Hospital

2 Department of Radiological Sciences, Ibaraki Prefectural University of Health Sciences

3 Department of Health Science, Graduate School of Medical Science, Kanazawa University

4 Department of Biotracer Medicine, Graduate School of Medical Science, Kanazawa University

For correspondence and reprints contact:
Hiroto YONEYAMA
Department of Radiological Technology, KanazawaUniversity Hospital, 13-1 Takara-machi, Kanazawa920-8641, JAPAN
Tel:81-76-265-2000
Fax:81-76-234-4311
E-mail address: kizu @cf6.so-net.ne.jp

Short running head: Optimizing SPECT/CT for SLNs

Abstract

Objective: Although SPECT/CT systems have been used for sentinel lymph node (SLN) imaging, few studies have focused on optimization of attenuation correction (AC) and scatter correction (SC). While SLNs could be detected in conventional planar images, they sometimes do not appear in SPECT/CT images. The purpose of this study was to investigate the optimal AC and SC and to improve the detectability of SLNs in examinations using SPECT/CT systems.

Materials and methods: The study group consisted of 56 female patients with breast cancer. In SPECT/CT imaging, four kinds of images were created with and without AC and SC; namely, AC-SC-, AC+SC-, AC-SC+ and AC+SC+. Five nuclear medicine physicians interpreted the planar and SPECT/CT images with five grades of confidence levels (1 to 5). The detection rate was calculated as the number of patients whose average confidence levels of interpretation were more than 4, divided by the total number of patients.

Results: The confidence level of interpretation and the detection rate provided by the planar images were 4.76 ± 0.49 and 94.6%, respectively. In

SPECT/CT imaging, the AC+SC- provided the best detection rate (confidence level of interpretation, 4.81 ± 0.38; detection rate, 98.2%), followed by the AC-SC- (4.70 ± 0.55, 89.3%), and the AC-SC+ (4.39 ± 1.2, 78.6%). The lowest values were obtained for the AC+SC+ (4.36 ± 1.22, 78.6%). Regarding the confidence levels of interpretation, significant differences were observed between AC+SC- and AC-SC-, AC+SC- and AC+SC+, AC+SC- and AC-SC+, and between planar images and AC+SC+ (P = 0.0021, 0.0009, 0.0013, and 0.0056, respectively).

Conclusions: When SPECT/CT was used, AC improved the detection of SLNs. SC caused disappearance of a faint SLN in some cases and should not be performed.

Key Words: *SPECT/CT, sentinel lymph node, attenuation correction, scatter correction, breast cancer*

INTRODUCTION

Visualization and localization of sentinel lymph nodes (SLNs) on lymphoscintigraphy is enhanced by the use of single-photon emission computed tomography/computed tomography (SPECT/CT) systems, particularly when drainage to lymph nodes is unpredictable, SLNs are close to the injection sites, extra-axillary SLNs are present, or SLNs are not identified on conventional planar images because of excessive soft tissue attenuation. Although detailed studies have been published on improvement of SLN localization with SPECT/CT systems [1-7], few studies have focused on attenuation correction (AC) and scatter correction (SC). Because of the scattering of gamma rays, it becomes difficult to identify the SLNs when they lie close to the injection sites. Since it is difficult to detect deeply situated SLNs because of the attenuation of gamma rays, we applied AC and SC. A faint SLN, however, sometimes disappeared in SPECT/CT images and the detectability of SLNs may worsen compared with that on planar images. Moreover, these corrections might cause artifacts near the injection sites. Thus, the purpose of this study was to investigate the optimal AC and SC and to improve the detection of SLNs in breast cancer patients.

MATERIALS AND METHODS

The study group consisted of 56 consecutive female patients (age, 56.1 ± 13.1 years) with histologically diagnosed breast cancer from November 2013 to July 2014. One patient was excluded because written informed consent was not obtained. Tumors were located on the right side in 22 cases and the left side in 32 cases, and were present on both sides in two cases. A 37 MBq (1mCi) dose of Technetium-99m (Tc-99m) phytate (FUJIFILM RI Pharma Co. Ltd., Japan) was injected subcutaneously around the tumor. Location markers containing 0.3 MBq (8.1μCi) of Tc-99m pertechnetate were placed at the center of the sternal notch and the xiphoid process. Planar imaging was performed at 10 min and 3－4 h after the injection. A dual -head gamma camera equipped with a low-to-medium energy general-purpose (LMEGP) collimator (Symbia T6; Siemens, Erlangen, Germany) was used for planar imaging. The counts in the planar image were acquired for 6 min in a 256 × 256 matrix with the LMEGP collimator. The injection sites were not covered with a lead shield. The energy was centered at 140 keV with a 20% window for Tc-99m. When the SLNs were not detected clearly such as at the

injection sites located near the axilla lymph nodes, the planar images were acquired from another direction. SPECT/CT imaging was performed after 3–4 h of planar imaging. The SPECT/CT system (Symbia T6; Siemens, Erlangen, Germany) used for imaging consisted of a dual-head gamma camera equipped with an LMEGP collimator and a multi-detector spiral CT optimized for rapid rotation. SPECT data were acquired in a 128 × 128 matrix for 20 sec each, for a total of 60 frames in steps of 6° over 360°. The energy was centered at 140 keV with a 15% window in SPECT/CT imaging. The scatter correction method was the dual energy window method [8,9]. The pixel truncation method was used to exclude the effects of high-level activity at the injection sites. The cutoff value was 100 counts in most cases, although it was changed as required in some cases. The data were reconstructed by using an iterative method based on an ordered subset expectation maximization algorithm with 12 iterations and 15 subsets using the resolution correction. A Gaussian filter was not used for smoothing. Four kinds of images were created with and without AC and SC; namely, AC-SC-, AC+SC-, AC-SC+ and AC+SC+. The attenuation coefficient was 0.15 cm^{-1}. A CT scan was obtained under the following conditions: tube voltage of 130 kV_p,

product of tube current and time of 50 mA, slice thickness of 2.5 mm, and reconstruction kernels of B35s kernel. Both SPECT and CT axial slices (slice thickness, 5 mm) were generated using the e.soft application package (Siemens), which was also used for fusing the CT and SPECT images. Maximum intensity projection (MIP) images were generated to identify the SLNs.

Interpretation of images

Five nuclear medicine physicians evaluated the planar and SPECT/CT images and recorded the degrees of confidence in interpreting the presence or absence of SLNs on images. The confidence levels of interpretation were evaluated using a five-grade scale: 1, definitely not identified; 2, probably not identified; 3, equivocal; 4, probably identified; and 5, definitely identified. The detection rate was calculated as the number of patients whose average confidence levels of interpretation were more than 4, divided by the total number of patients. The confidence levels among the planar images and the SPECT/CT images (AC+SC+, AC-SC-, AC+SC-, and AC-SC+) were compared using the Wilcoxon signed-rank test. Statistical significance was defined as $p < 0.01$. Regions of interest were placed on SLNs

in SPECT/CT images. We compared the counts of SLNs among AC+SC+, AC-SC-, AC+SC-, and AC-SC+. The effect of SC was evaluated using the following equation: effect of SC = (the counts decreased by the SC) × 100 / (the counts obtained without SC). The effect of AC was evaluated using the following equation: effect of AC = (the counts increased by the AC) × 100 / (the counts obtained without AC). Before examination, approval for the study protocol was obtained from the institution's ethical committee and written informed consent was obtained from the patients.

RESULTS

The confidence levels of interpretation and the detection rate provided by the planar images were 4.78 ± 0.49 and 94.6%, respectively. The confidence levels of interpretation and the detection rate in planar and SPECT/CT images are shown in Fig. 1 and Table 1. The detection rate provided by the AC+SC- was the best (confidence level of interpretation, 4.81 ± 0.38; detection rate, 98.2%), followed by the AC-SC- (4.70 ± 0.55, 89.3%), and the AC-SC+ (4.39 ± 1.17, 78.6%). The values for the AC+SC+ were the lowest (4.36 ± 1.22, 78.6%). Significant differences were observed between

AC+SC- and AC-SC-, AC+SC- and AC+SC+, AC+SC- and AC-SC+, and between planar images and AC+SC+ (P = 0.0021, 0.0009, 0.0013, and 0.0056, respectively). The SLN count provided by the AC+SC- was the highest (11426 ± 14214; median, 6123 counts), followed by those of the AC+SC+ (8869 ± 14408; median, 3135 counts), and the AC-SC- (4904 ± 5833; median, 2924 counts). The AC-SC+ counts were the lowest (3804 ± 5854; median, 1884 counts) (Table 2). The average distance from SLNs to the body surface was 2.6 ± 1.3 cm (median, 2.2 cm). The distance from SLNs to body surface and an effect of AC have a fair correlation (R^2 = 0.464) (Fig. 2). The counts of SLNs, especially deeply situated SLNs, increased when using the AC. When the nodes were close to the body surface, the effects of AC were less significant. In some cases, an artifact occurred as a result of the AC on the border of the lung and the breast. The average distance from injection sites to SLNs was 7.6 ± 2.6 cm (median, 7.3 cm). The distance from injection sites to SLNs and the effect of the SC showed a fair correlation (R^2 = 0.433) (Fig. 3). The counts of SLNs decreased when using the SC, especially near the injection sites. A faint SLN disappeared as a result of the SC (Fig. 4). The counts of SLNs increased when using the AC, especially in deeply

situated SLNs (Fig. 5). In one case, while SLNs could not be detected clearly in both the planar image and the SPECT/CT fused image, these lymph nodes could be identified with the gamma probe during surgery (Fig. 6). Since the SLNs could not be clearly detected in the planar image at 3 hours after injection, the SPECT/CT images were acquired after confirming regional movement by massage of injection sites (Fig. 7). The anatomical information of the CT made a precise localization of the SLNs possible. The SPECT/CT images helped to rule out artifacts from the injection site and questionable contamination, which was sometimes seen during injection. Although the SLNs near injection sites could not be clearly identified in the planar image, they were identified in the SPECT/CT fused images (Fig. 8).

DISCUSSION

Many researchers have reported that the SPECT/CT provided additional value in determination of the exact anatomic location of sentinel nodes for the successful identification of SLNs. Even-Sapir et al. reported that SPECT/CT SLN mapping provided additional data that are of clinical relevance to SLN biopsy and added clinically relevant data for 4 of 9 patients

with head and neck tumor and 6 of 12 patients with trunk melanoma [10]. Van der Ploeg et al. showed that SPECT/CT enabled the visualization of drainage in patients in whom planar imaging did not detect SLNs. These authors reported that SPECT/CT enabled visualization of lymphatic drainage in 123 (92%) of 134 patients [11]. Lerman et al. reported that the difference between SLN detection by planar imaging and SLN detection by SPECT/CT in overweight and obese patients was statistically significant. SPECT/CT identified hot nodes in 91% of the study cohort, including 29 patients for whom planar imaging failed to detect hot nodes [12]. They also reported that planar imaging alone was negative for identification of hot nodes in 15% of the patients. SPECT/CT alone was negative in 10% and both techniques were negative in 9% of the patients. Forty-six of a total of 361 (13%) hot nodes identified by lymphoscintigraphy were detected only on SPECT/CT, including 21 nodes obscured by the scattered radiation from the injection sites [13].

Image quality is greatly affected by scattered radiation because injection sites with high levels of radioactivity exist near the lymph node with low levels of radioactivity. Additionally, SPECT/CT systems provide an

accurate AC of the nuclear medicine image data [14]. Therefore, we have applied AC and SC to improve the detectability. However, in our experience, although the SLNs could be detected in planar images, they sometimes disappeared in SPECT/CT images. These corrections may even cause artifacts near the injection sites. The counts of SLNs increased when using the AC, especially deeply situated SLNs. Our results showed that AC might improve the detection of SLNs, especially for deeply situated SLNs. When the nodes are close to the body surface, the effect of AC was relatively small. The counts of SLNs decreased when using the SC, especially near the injection sites. A faint SLN near injection sites might disappear because of the SC. When SC was applied, an SLN became invisible in some cases. Therefore, we do not recommend that SC is performed. The high detection rate and high confidence levels of interpretation suggest that AC+SC- was the optimal combination of AC and SC. At the confidence levels of interpretation, a significant difference was not observed between AC+SC- and planar images. We need to perform both planar imaging and SPECT/CT imaging for better visualization and localization of SLNs. Although the AC caused artifacts on the border of the lung and the breast, the SPECT/CT

images could rule out these artifacts.

In one case, SLNs could not be detected in both the planar image and the SPECT/CT fused image, but could be identified with the gamma probe during surgery. Williams et al. reported that some SLNs may not be visualized until late in the study. Exercise or muscle contractions could facilitate lymphatic flow. Even when regional movement of the affected limb causes stagnation in the injection sites, such procedures can improve the lymphatic flow [15]. Histopathologic examination detected metastasis in the SLNs that were not detected in lymphoscintigraphy. Noguchi reported that the SLN counts in metastasis-positive lymph nodes were significantly lower than that those in metastasis-negative lymph nodes [16].

When the SLNs are located close to the injection sites, techniques for reducing the artifacts from the injection sites are important. Therefore, we applied the pixel truncation method [17] and the ordered subset expectation maximization reconstruction algorithm [18]. These techniques reduce the artifacts in scintigraphy. We used the LMEGP collimator for reducing the star-shaped artifacts. The LMEGP collimator improved the detection of SLNs, particularly in SLNs located close to the injection sites

compared with the low-energy high-resolution (LEHR) collimator [19]. Recently, resolution correction has been performed for SPECT reconstruction [20-22]. When the resolution correction was applied, the resolutions of LMEGP and LEHR became similar. We therefore recommend routine use of LEMGP collimator for lymphoscintigraphy with SPECT/CT systems.

CONCLUSION

AC improved the detection of SLNs. SC should not be performed because it occasionally caused a faint SLN to become invisible. The combination with AC and without SC was recommended to improve the detectability, because of the high detection rate and the high confidence levels of interpretation.

ACKNOWLEDGMENT

This work was supported by Grants-in-Aid for Scientific Research in Japan (No.25931050). The authors thank N. Akatani, T. Yamase,Y. Kunida and all the nuclear medicine physicians at Kanazawa University Hospital for their interpretation of lymphoscintigraphy images. We are grateful to M. Tobisaka, M. Kawamura, K. Noto, and all the radiological technologists at Kanazawa University Hospital for providing technical support.

REFERENCES

1. van der Ploeg IM, Valdes Olmos RA, Nieweg OE, Rutgers EJ, Kroon BB, Hoefnagel CA. The additional value of SPECT/CT in lymphatic mapping in breast cancer and melanoma. J Nucl Med. 2007;48:1756-60.
2. Husarik DB, Steinert HC. Single-photon emission computed tomography/computed tomographyfor sentinel node mapping in breast cancer. Semin Nucl Med. 2007;37:29-33.
3. van der Ploeg IM, Olmos RA, Kroon BB, Rutgers EJ, Nieweg OE. The hidden sentinel node and SPECT/CT in breast cancer patients. Eur J Nucl Med Mol Imaging. 2009;36:6-11.
4. Buck AK, Nekolla S, Ziegler S, Beer A, Krause BJ, Herrmann K, et al. SPECT/CT. J Nucl Med. 2008;49:1305-19.
5. Mariani G, Bruselli L, Kuwert T, Kim EE, Flotats A, Israel O, et al. A review on the clinical uses of SPECT/CT. Eur J Nucl Med Mol Imaging. 2010;37:1959-85.
6. Laetitia V, Ohnona J, Groheux D, Slama A, Colletti PM, Chondrogiannis S, et al. Role of SPECT/CT in sentinel lymph node detection in patients with breast cancer. Clin Nucl Med. 2014;39:431-6.
7. Moncayo VM, Aarsvold JN, Grant SF, Bartley SC, Alazraki NP. Status of sentinel lymph node for breast cancer. Semin Nucl Med. 2013;43:281-93.
8. Sadrmomtaz A, Asl MN. Reliability of scatter correction methods in SPECT by setting two energy windows. World Applied Programming. 2011;1:143-9.
9. de Nijs R, Lagerburg V, Klausen TL, Holm S. Improving quantitative dosimetry in (177)Lu-DOTATATE SPECT by energy window-based scatter corrections. Nucl Med Commun. 2014;35:522-33.
10. Even-Sapir E, Lerman H, Lievshitz G, Khafif A, Fliss DM, Schwartz A, et al. Lymphoscintigraphy for sentinel node mapping using a hybrid SPECT/CT system. J Nucl Med. 2003;44:1413-20.
11. van der Ploeg IM, Nieweg OE, Kroon BB, Rutgers EJ, Baas-Vrancken Peeters MJ, Vogel WV, et al. The yield of SPECT/CT for anatomical lymphatic mapping in patients with breast cancer. Eur J Nucl Med Mol Imaging. 2009;36:903-9.
12. Lerman H, Lievshitz G, Zak O, Metser U, Schneebaum S, Even-Sapir E. Improved sentinel node identification by SPECT/CT in overweight patients with breast cancer. J Nucl Med. 2007;48:201-6.
13. Lerman H, Metser U, Lievshitz G, Sperber F, Shneebaum S, Even-Sapir E. Lymphoscintigraphic sentinel node identification in patients with breast cancer: the role of SPECT-CT. Eur J Nucl Med Mol Imaging. 2006;33:329-37.

14. Patton JA, Turkington TG. SPECT/CT physical principles and attenuation correction. J Nucl Med Technol. 2008;36:1-10.
15. S.Williams B, Hinkle GH, Douthit RA, Fry JP, Pozderac RV, Olsen JO. Lymphoscintigraphy and intraoperative lymphatic mapping of sentinel lymph nodes in melanoma patients. J Nucl Med Technol. 1999;27:309-17.
16. Noguchi A, Onoguchi M, Ohnishi T, Hashizume T, Kajita A, Funauchi M, et al. Predicting sentinel lymph node metastasis in breast cancer with lymphoscintigraphy. Ann Nucl Med. 2011;25:221-6.
17. Funahashi M, Shimonagata T, Mihara K, Kashiyama K, Shimizu R, Machida S, et al. Application of pixel truncation to reduce intensity artifacts in myocardial SPECT imaging with Tc-99m tetrofosmin. J Nucl Cardiol. 2002;9:622-31.
18. Leong LK, Kruger RL, O'Connor MK. A comparison of the uniformity requirements for SPECT Image reconstruction using FBP and OSEM techniques. J Nucl Med Technol. 2001;29:79-83.
19. Yoneyama H, Tsushima H, Kobayashi M, Onoguchi M, Nakajima K, Kinuya S. Improved detection of sentinel lymph nodes in SPECT/CT images acquired using a low-to medium-energy general-purpose collimator. Clin Nucl Med. 2014;39:e1-6.
20. Yokoi T, Shinohara H, Onishi H. Performance evaluation of OSEM reconstruction algorithm incorporating three-dimensional distance-dependent resolution compensation for brain SPECT: A simulation study. Ann Nucl Med. 2002;16:11-8.
21. Takahashi Y, Murase K, Mochizuki T, Sugawara Y, Maeda H, Kinda A. Simultaneous 3-dimensional resolution correction in SPECT reconstruction with an ordered-subsets expectation maximization algorithm. J Nucl Med Technol. 2007;35:34-8.
22. Okuda K, Nakajima K, Yamada M, Wakabayashi H, Ichikawa H, Arai H, et al. Optimization of iterative reconstruction parameters with attenuation correction, scatter correction and resolution recovery in myocardial perfusion SPECT/CT. Ann Nucl Med. 2014;28:60-8.

Legends for illustrations

Table 1 Detection rate for sentinel lymph nodes in planar and SPECT/CT images with and without attenuation correction and scatter correction.

Table 2 Average counts (mean ± standard deviation: SD) of SLNs in SPECT/CT images with and without attenuation correction and scatter correction.

Fig. 1 Comparison of confidence levels of interpretation in planar and SPECT/CT images with and without attenuation correction (AC) and scatter correction (SC).

Fig. 2 Relation between distance from SLNs to body surface and effect of the attenuation correction.

Fig. 3 Relation between distance from injection sites to SLNs and effect of the scatter correction.

Fig. 4 SPECT/CT fused images and maximum-intensity projection (MIP) images of a 77-year-old female patient. The SPECT/CT (A) and MIP (B) images with AC+SC+, AC-SC+ (C, D), AC+SC- (E, F), and AC-SC- (G, H).

A planar image obtained 3 hours after injection (I).

Fig. 5 SPECT/CT fused images and maximum intensity projection (MIP) images of a 79-year-old female patient. The SPECT/CT (A) and MIP (B) images with AC+SC+, AC-SC+ (C, D), AC+SC- (E, F), and AC-SC- (G, H).

A planar image obtained 3 hours after injection (I).

Fig. 6　A planar image of a 71-year-old female patients. Although SLNs could not be clearly detected in lymphoscintigraphy, they could be identified with the gamma probe during surgery.

Fig. 7　A planar image and SPECT/CT fused images of a 67-year-old female patient. Although axillary SLNs near injection sites could not be clearly detected in the planar image obtained 3 hours after injection (A), they could be detected in the planar image obtained 4 hours after injection (D). They could not be detected using SPECT/CT fused image with AC-SC+ (B) and AC+SC+ (C) obtained 4 hours after injection, but they were detected using SPECT/CT fused image with AC+SC- (E) and AC-SC- (F) obtained 4 hours after injection.

Fig. 8　A planar image and SPECT/CT fused images of a 73-year-old female patient. Although axillary SLNs near injection sites could not be clearly detected in the planar image (A) and the SPECT/CT fused image with AC-SC+ (B) and AC+SC+ (C), they were detected using SPECT/CT fused image with AC+SC- (D) and AC-SC- (E).

Table1 Detection rate for SLNs in planar and SPECT/CT images.

	SPECT/CT		Planar
	With attenuation correction	Without attenuation correction	
With scatter correction	78.6% (44/56)	78.6% (44/56)	94.6%
Without scatter correction	98.2% (55/56)	89.3% (50/56)	(53/56)

Table2　Average counts of SLNs in SPECT/CT images.

	With attenuation correction	Without attenuation correction
With scatter correction	8869 ± 14408	3804 ± 5854
	Median 3135	Median 1884
Without scatter correction	11426 ± 14214	4904 ± 5833
	Median 6123	Median 2924

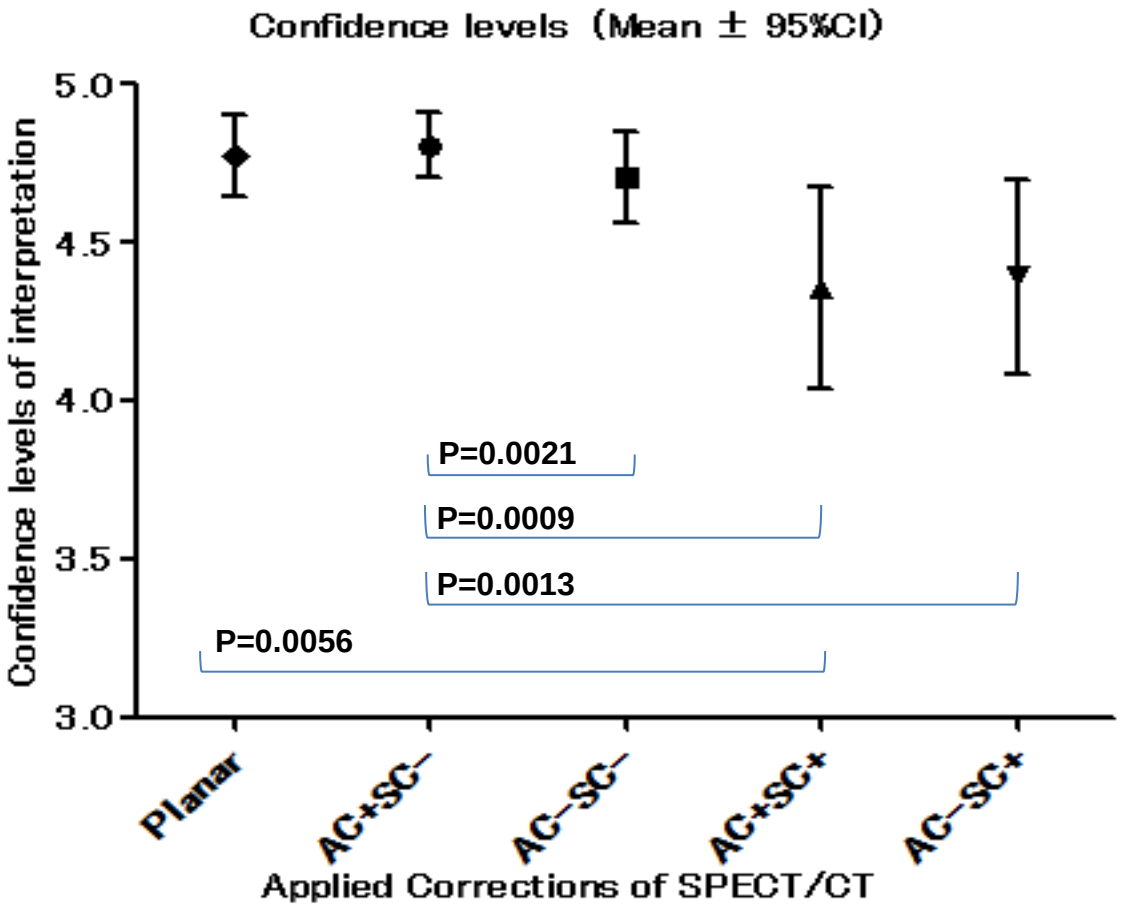
Confidence levels (Mean ± 95%CI)
Confidence levels of interpretation
5.0
4.5
4.0
3.5
3.0
P=0.0021
P=0.0009
P=0.0013
P=0.0056
Planar
AC+SC-
AC-SC-
AC+SC+
AC-SC+
Applied Corrections of SPECT/CT

Fig. 1

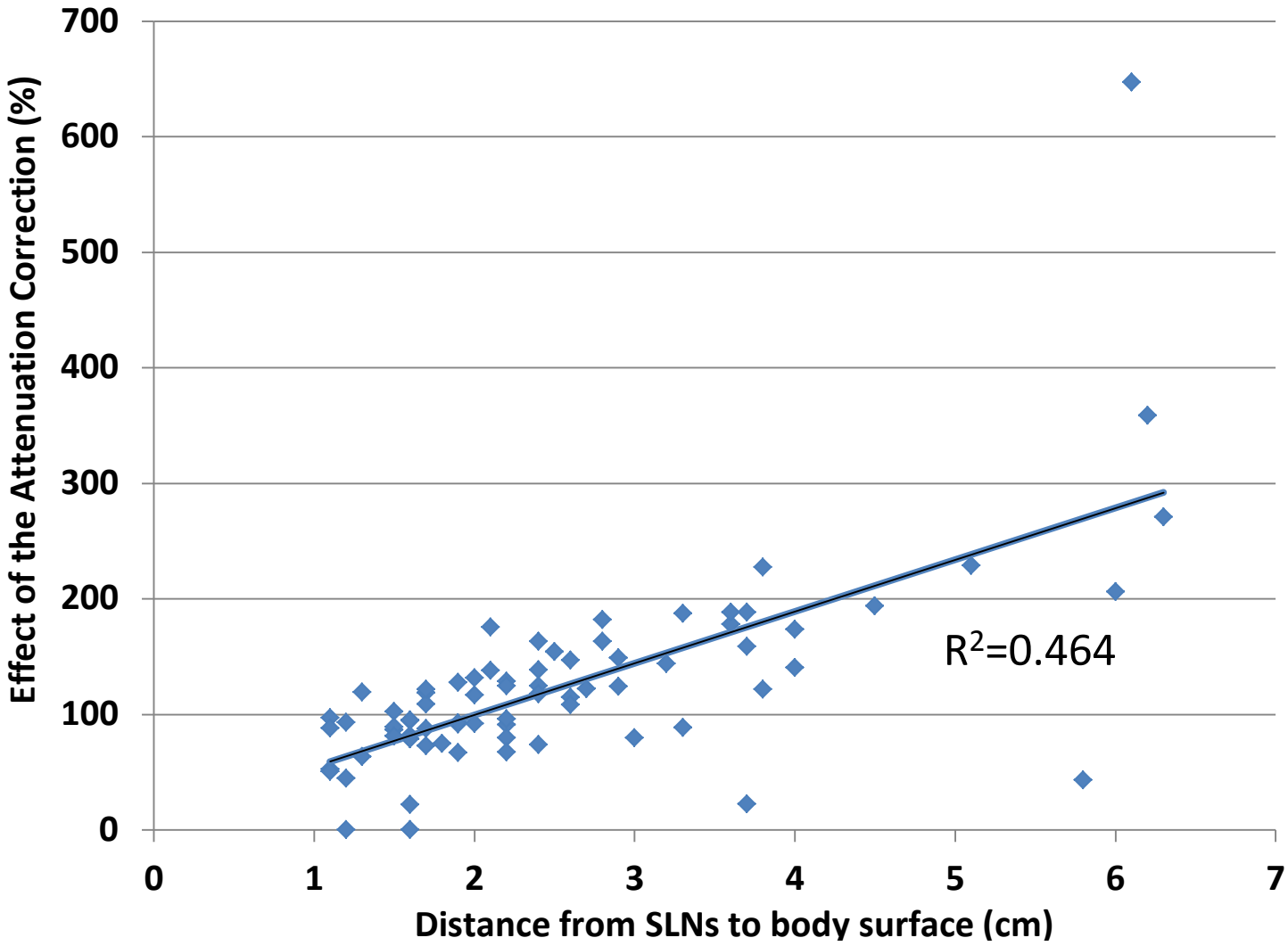
Effect of the Attenuation Correction (%)
700
600
500
400
300
200
100
0
0
1
2
3
4
5
6
7
Distance from SLNs to body surface (cm)
R2=0.464

Fig. 2

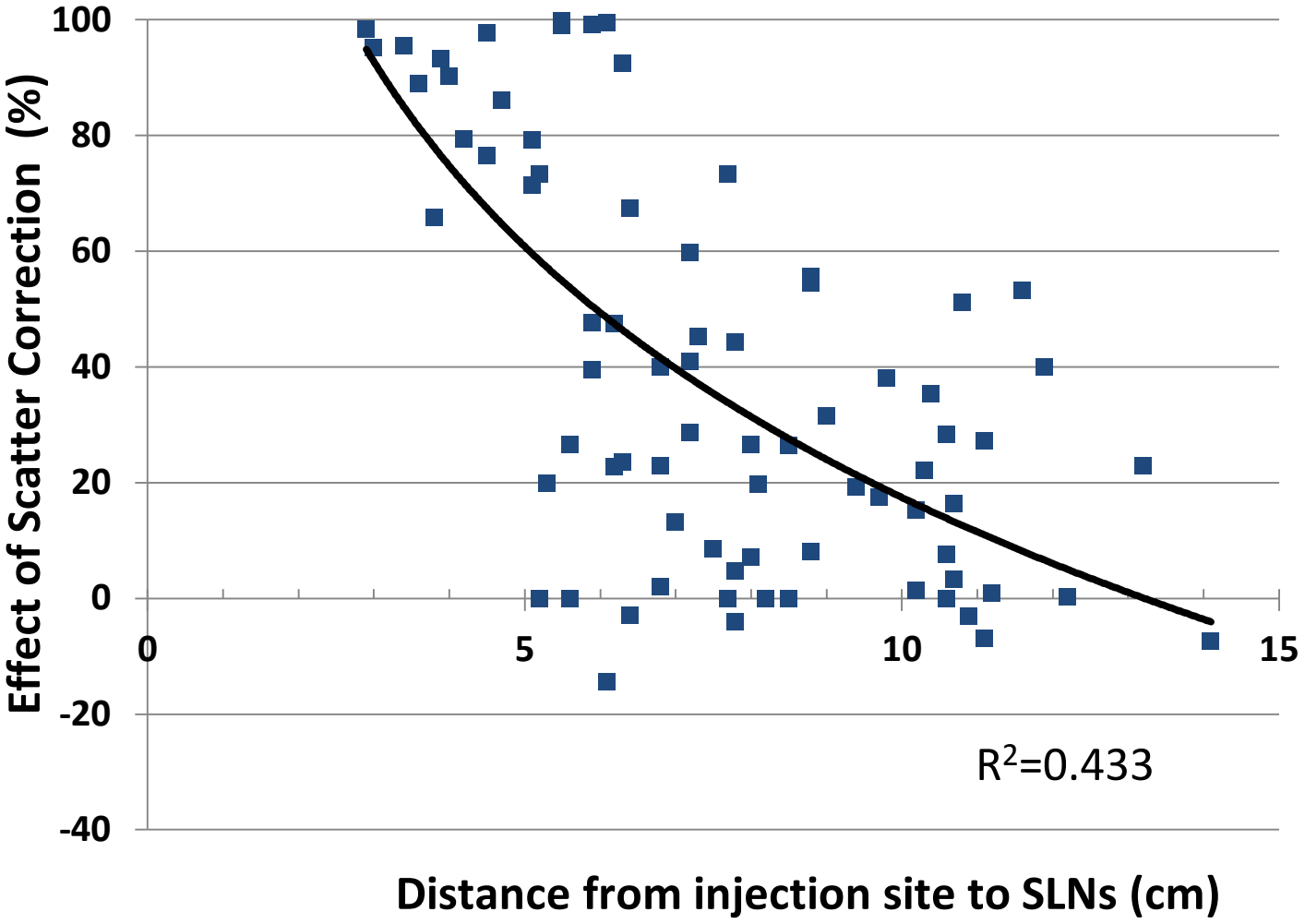
100
80
60
40
20
0
-20
-40
0
5
10
15
Effect of Scatter Correction (%)
Distance from injection site to SLNs (cm)
R2=0.433

Fig. 3

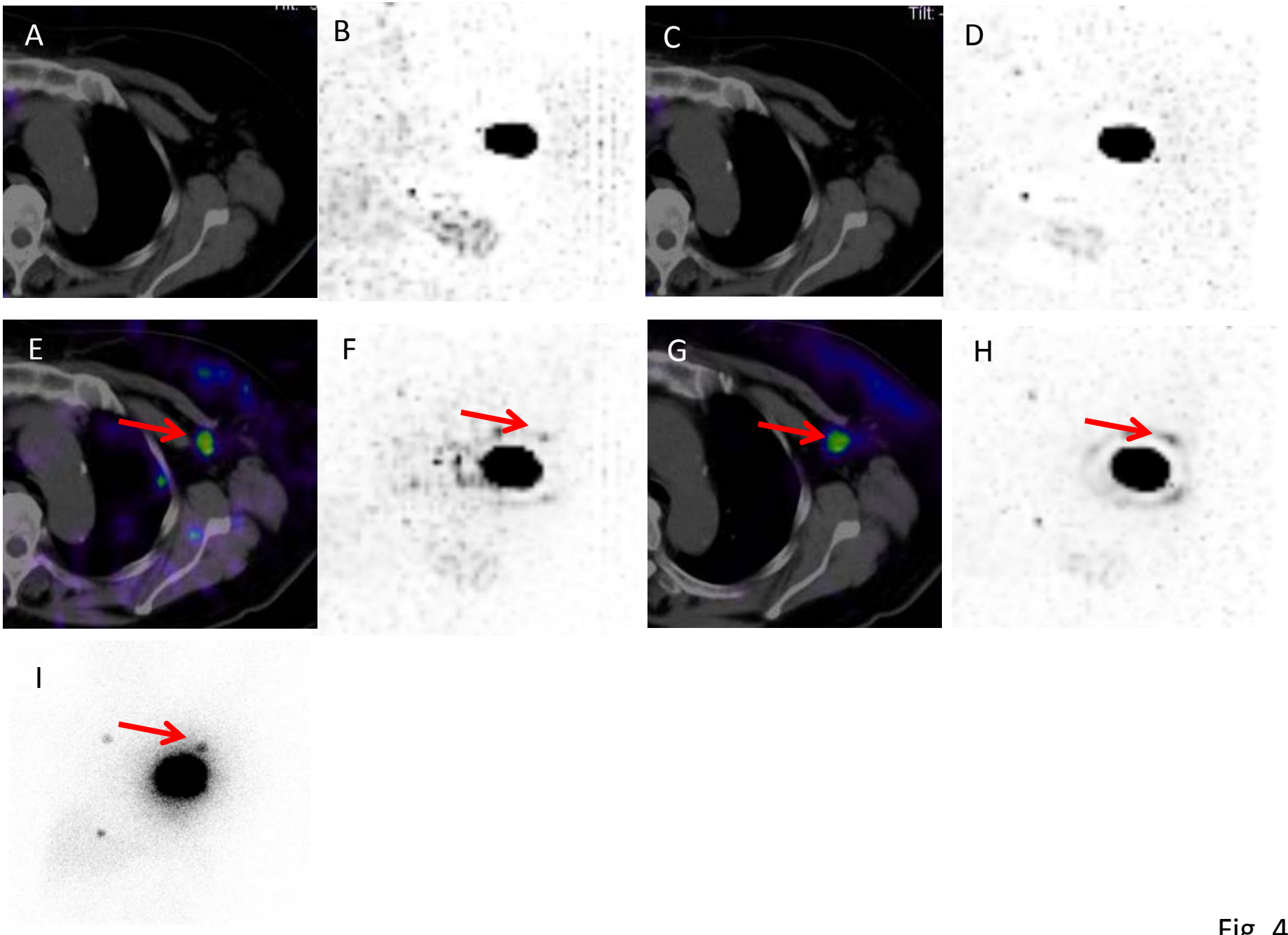

Fig. 4

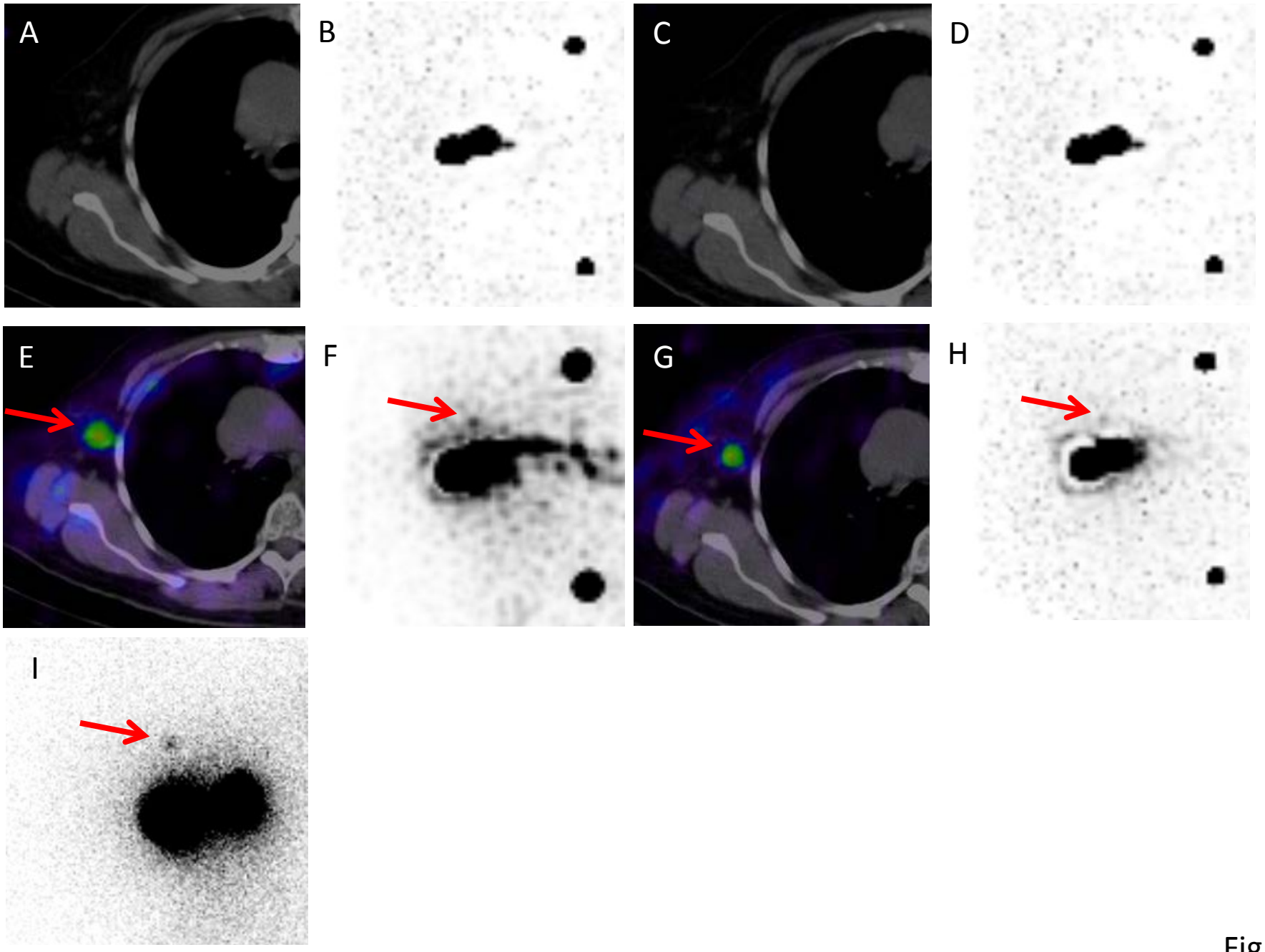

Fig. 5

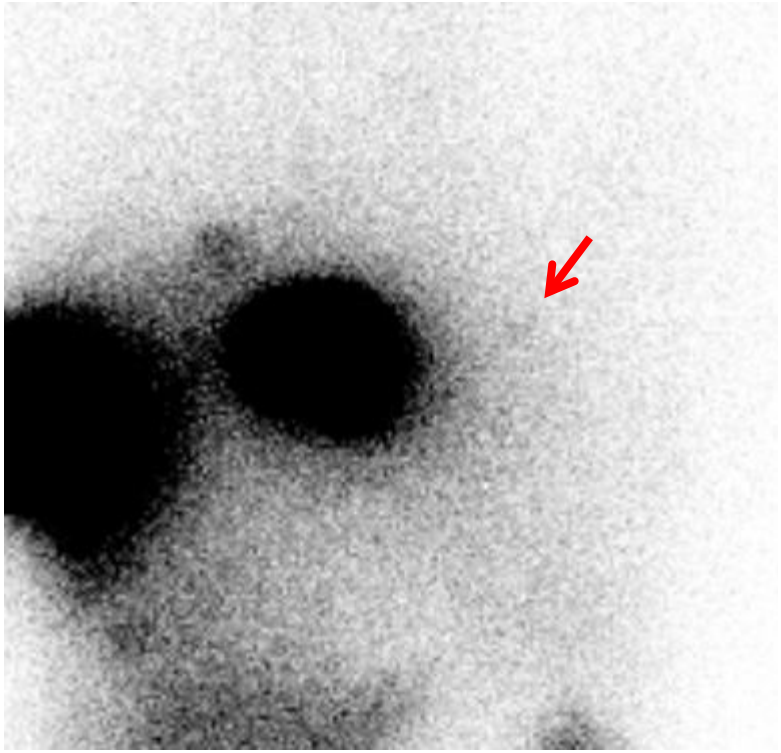

Fig. 6

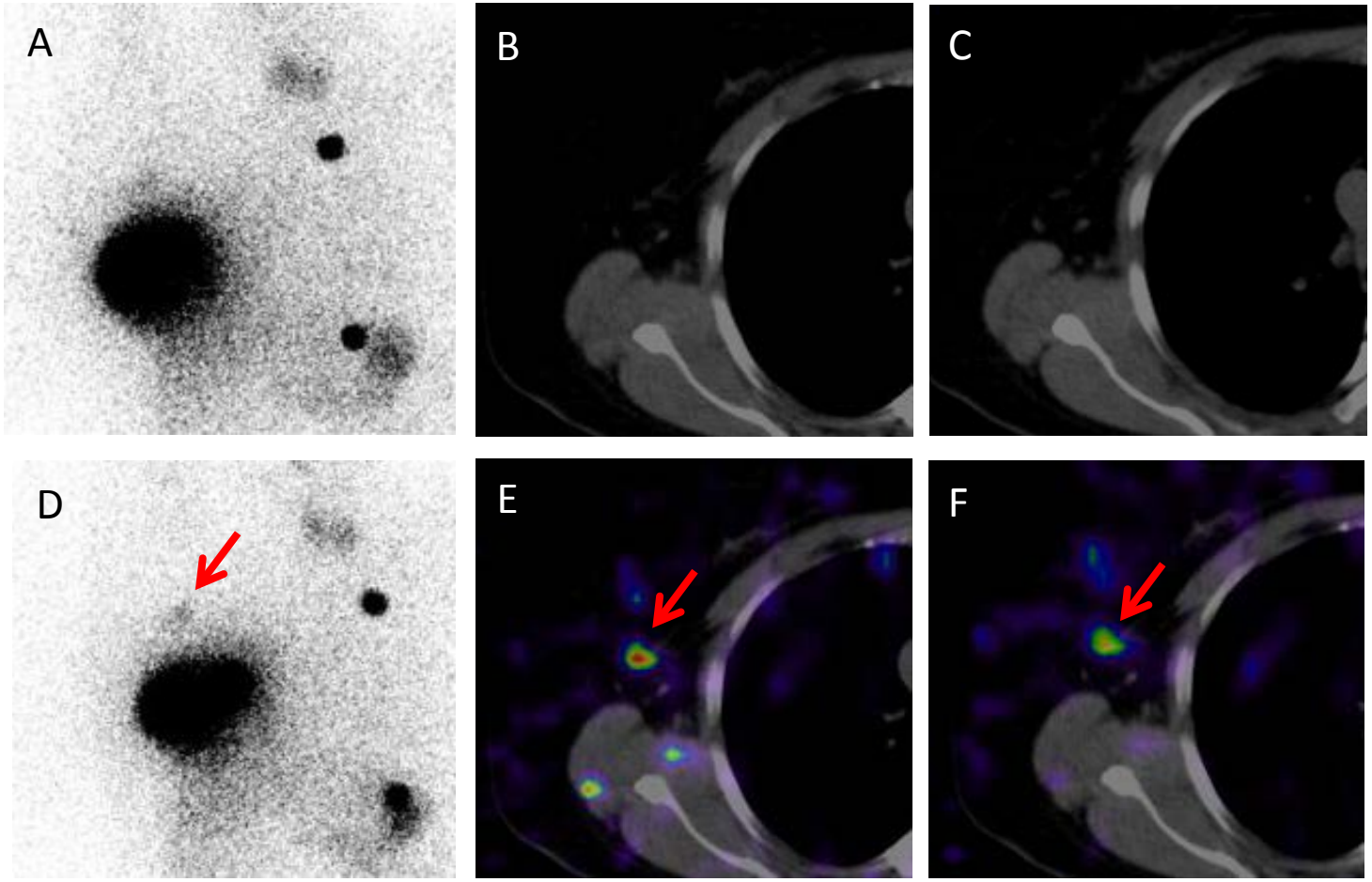

Fig. 7

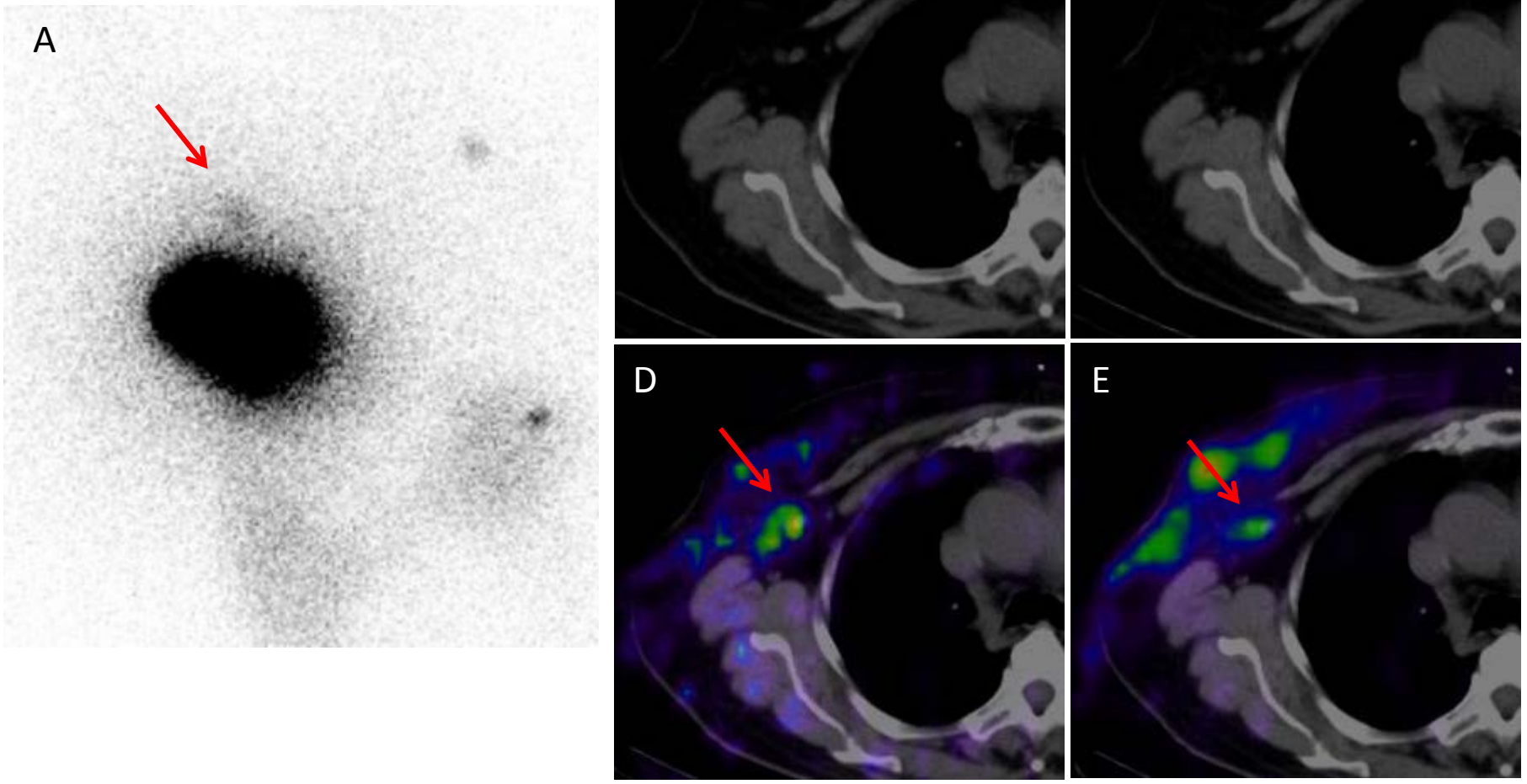

Fig. 8